



Catalytic activity of Fe-modified bentonite in heterogeneous photo-Fenton process

Simin Khoroushi Isalou, Mohammad Ghorbanpour*

Department of Chemical Engineering, University of Mohaghegh Ardabili, Ardabil, Iran, emails: Ghorbanpour@uma.ac.ir (M. Ghorbanpour), khoroushi.s@gmail.com (S.K. Isalou)

Received 19 November 2018; Accepted 12 April 2019

ABSTRACT

In this study, an easy and inexpensive approach is introduced to synthesize Fe-modified clays for industrial applications. A novel heterogeneous photo-Fenton catalyst was prepared by solid-state ion exchange method. Synthesis of Fe-modified bentonite (Fe-B) was performed at 100°C and 200°C for 0.5, 1, and 2 min. Fe-B was characterized by scanning electron microscopy, elemental dispersive X-ray spectroscopy and X-ray diffraction. The activity of prepared Fe-B catalyst was evaluated in the degradation of methylene blue (MB) in the presence of H₂O₂ and under UV irradiation. The effects of reaction parameters such as initial dye concentration, H₂O₂ concentration, Fe-B catalyst loading and initial solution pH on the degradation of MB were also investigated. Between different prepared Fe-B catalysts, the sample prepared at 100°C and 2 min was selected as the optimum conditions for synthesis. Under optimal conditions (pH = 4.0 and 200 ppm H₂O₂), ~100% discoloration of 200 ppm MB can be achieved in 90 min. The result of two reusability studies on the catalyst for the decolorization of MB was 93.8% and 90.5% after 1st and 2nd reuse, respectively. The result of reusability studies shows the acceptable reusability of the catalyst. These results were satisfactory to recommend Fe-modified bentonite prepared by solid-state ion exchange method as a novel catalyst.

Keywords: Discoloration; Fe-modified bentonite; Solid-state ion exchange; Photo-Fenton

1. Introduction

Industrial, agricultural, and domestic wastes have contributed to the contamination of water sources with several organic, severely toxic and non-biodegradable compounds. As modern health-quality standards and environmental regulations are becoming gradually more restrictive, such wastewaters have been realized as a major social and economic problem. Many persistent organic chemicals in water (pesticides, dyes or similar refractory compounds) cannot be removed by conventional biotechnological, physical or chemical processes due to a high operating cost and/or the production of waste water or residues that are difficult to handle. As an alternative methods, advanced oxidation processes (AOP) based on the action of hydroxyl radicals

([•]OH) enable almost complete mineralization of organic matter using milder experimental conditions [1,2]. One of the most important AOP processes for the generation of hydroxyl radicals is based on the combined action of Fe²⁺/H₂O₂/UV radiation in the so called homogeneous photo-Fenton process, as Fe²⁺ ions are supplied in aqueous solution.

Photo-Fenton oxidation processes are environmentally friendly, since they do not involve the use of harmful chemical reagents. Moreover such methods are easy to handle and can be operated using quite uncomplicated reactor designs. Homogeneous-Fenton reaction has been considered as one of the most efficient routes for the treatment of water polluted with recalcitrant chemicals in the last decades [3]. The homogeneous photo-Fenton process requires complementary steps to recover the catalyst, prevent contamination

* Corresponding author.

and enable catalyst re-use, such as precipitation and re-dissolution; thus the cost of the homogeneous processes largely depends on the supply of chemicals, power and labour requirements [4,5]. The heterogeneous photo-Fenton reaction overcomes these disadvantages. Several attempts have been made to develop support catalysts as heterogeneous catalyst using silica gel [4,6], clay [2,7–9], graphite [10,11] and activated carbon [12,13].

The first and most common method for the preparation of Fe-modified clays is the ion exchange process [1,3,4]. For example, Bossmann et al. prepared Fe (III)-doped zeolite Y catalyst through a simple ion exchange reaction (Fe^{3+} vs. Na^+) and used it as a suspended photo-Fenton catalyst for the degradation of polyvinyl alcohol [14]. However, this catalyst exhibited a very poor catalytic activity since, the dissolved organic carbon remains at a high level after 120 min reaction. Another common method in the preparation of Fe-modified clays is the pillaring which is comprised of the following three steps: polycation synthesizing by polymerization; intercalation of the polycation into layer space of the clay; and finally, applying heat treatment. When heated to a temperature greater than 300°C , the intercalated metal hydroxy cations undergo dehydration and dehydroxylation and are converted by metal oxide clusters acting as pillars, thus creating a stable microporous system in the interlamellar space of clay particles clay [15–18]. The negative outcome of the ion exchange process is its lengthy processing and multistep preparation procedures.

In this research a new method called “solid-state ion exchange method” was applied to resolve these problems. In solid-state ion exchange method, iron salt is mixed with bentonite at solid-state and heated at around the melting point of iron salt. Synchronized application of heat and ion exchange creates a fast process. Furthermore, under the common procedure, the usual temperature is 300°C , while in this research the reaction was accomplished at melting point of iron chloride, that is, $\sim 100^\circ\text{C}$. Briefly, an easy and inexpensive approach is introduced to synthesize Fe-modified clays for industrial applications. Recently, the application of solid-state ion exchanged clay is reported in the antibacterial and adsorption applications [19–22]. These modified clays exhibited high antibacterial activity, good stability and low cost. The aim of this study was to synthesize Fe-modified bentonite (Fe-B) by solid ion exchange and then characterize and evaluate their photocatalytic activity. As far as this study is concerned, the catalytic activity of Fe-B composites prepared via solid-state ion exchange method in heterogeneous photo-fenton process has never been reported in the literature.

2. Material and methods

2.1. Material

Bentonite clay (Ca-montmorillonite) was obtained from Kanisaz Jam Company (Rasht, Iran). Iron chloride ($\text{FeCl}_2 \cdot 4\text{H}_2\text{O}$), sodium hydroxide (NaOH), chloride acid (HCl), hydrogen peroxide (H_2O_2 , 30% w/w) and methylene blue (MB) were purchased from Merck Company, (Germany). All the chemicals were of reagent grade and used without further purification and the solutions were prepared with deionized water.

2.2. Preparation of Fe-B

$\text{FeCl}_2 \cdot 4\text{H}_2\text{O}$ (1 g) and bentonite (1 g) were completely mixed in solid-state form. This mixture were placed in a furnace at 100° and 200°C for 0.5, 1, and 2 min. Then, the samples were removed from the furnace, adequately washed with distilled water, filtered and dried in an oven at 25°C for 24 h. The Fe-B nanocomposites prepared at 100°C for 0.5, 1, and 2 min and prepared at 200°C for 0.5, 1, and 2 min was named as samples 1 to 6 respectively.

2.3. Characterization

Scanning electron microscopy (SEM) and elemental dispersive X-ray spectroscopy (EDX) analysis were obtained with an LEO 1430VP instrument. X-ray diffraction (XRD) patterns of the samples were characterized using an X-ray diffractometer (Philips PW 1050, Netherlands) with $\text{CuK}\alpha$ radiation ($\lambda = 1.5418 \text{ \AA}$, 40 kV and 30 mA, 2θ from 4° to 80° and 0.05° step).

2.4. Activity tests

The photo-catalytic oxidation experiments were carried out in a 250 mL Pyrex open vessel, placed on a magnetic stirrer and under UVC-lamps (4 W, Philips). The distance between the solution and the UV source was kept constant at 15 cm, in all experiments. After stabilization of the stirring speed ~ 350 rpm and $\text{pH} = 4$, the Fe-B was introduced into the vessel containing 100 mL of the aqueous solution of MB. Then 8 mM of H_2O_2 was added to the reaction vessel. The moment of adding H_2O_2 was considered as the initial time for reaction. The solution was subsequently stirred for 2 h. During the reaction, liquid aliquots were retrieved from the vessel at selected time intervals. Residual H_2O_2 in these samples was immediately quenched with MnO_2 , in order to avoid the occurrence of dark Fenton reaction through the possible presence of leached iron. Before analysis, liquid was centrifuged. Dye removal efficiency was calculated as follows:

$$\text{Discoloration efficiency} = \left[\frac{C_0 - C_t}{C_0} \right] \times 100\% \quad (1)$$

where C_0 and C_t (mg L^{-1}) are the liquid-phase concentration of the MB at the initial and any time t respectively, measured by UV VIS-spectrophotometer (Nanalytic, Germany).

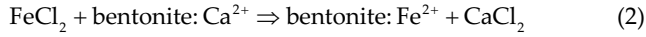
2.5. Catalyst reusability test

For stability test, the catalysts were tested in three different consecutive experiments using fresh dye solution at the best observed experimental conditions. After each experimental runs, the applied catalyst was filtered, washed with distilled water and dried in the oven at 25°C for 24 h.

3. Results and discussion

The expected chemical reaction occurred during the molten solution of FeCl_2 contact with bentonite. The high temperature prompted the ion exchange reaction by diffusion

of present Fe in the molten salt of iron chloride and calcium of bentonite matrix. The chemical reaction is represented as follows:



Moreover, calcinations of obtained bentonite: Fe²⁺ resulted in the formation of the Fe_xO_y particles.



3.1. Morphology

The image of SEM of bentonite and Fe-B is presented in Fig. 1. The SEM image of parent bentonite (Fig. 1a) shows a layered structure with a typical sheet-like morphology. After the solid-state ion exchange, the original structure of bentonite remains. The only observed difference is the slight opening of the flakes. Interestingly, after these ion exchange-based methods, no particles can be seen on the bentonite surface. This is because of very small size of Fe_xO_y particles (smaller than 2 nm) which present in the interlayer

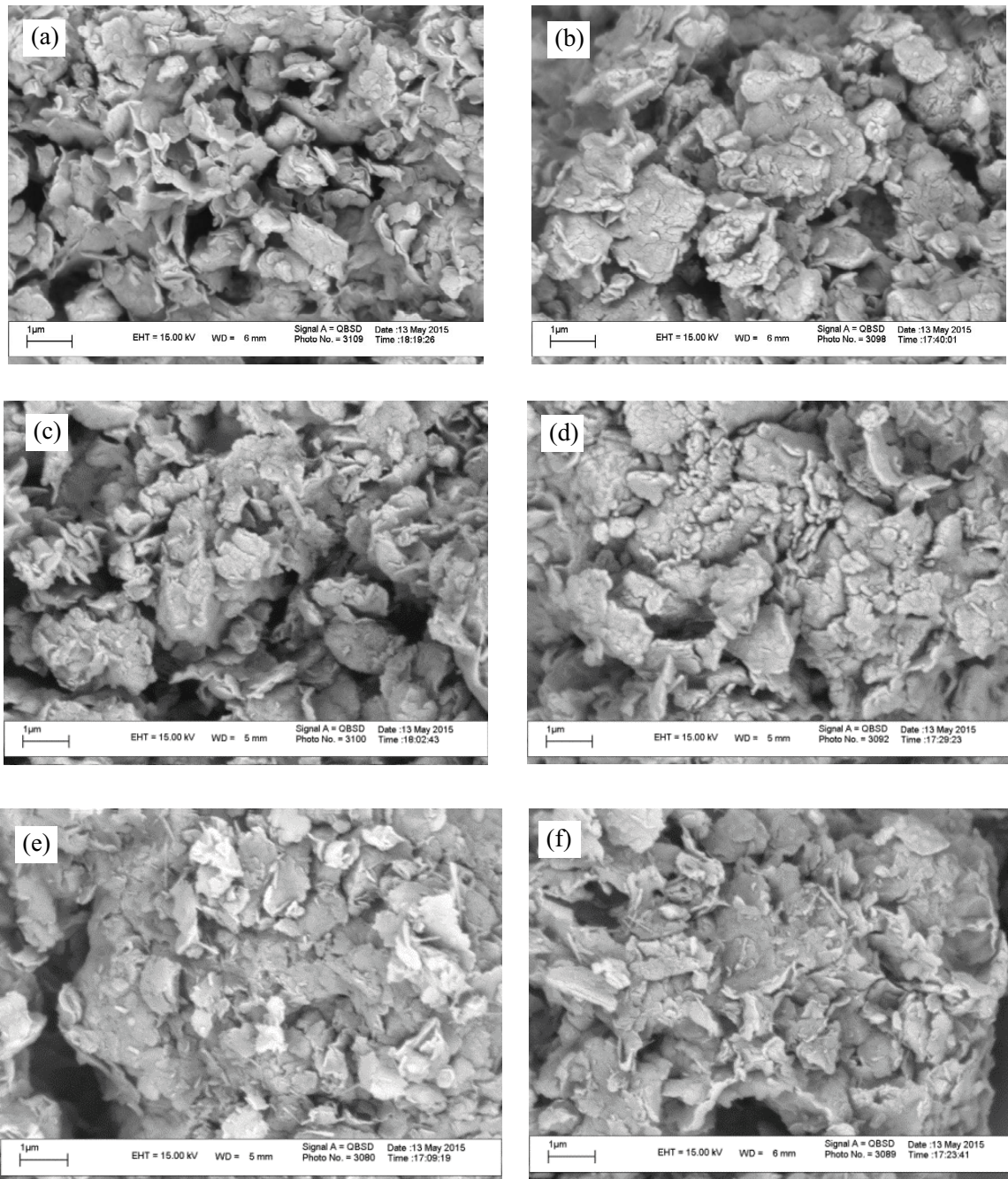


Fig. 1. SEM images of (a) Bentonite and bentonite/iron nanocomposites prepared at 100°C for 1 (b) and 2 (c) minutes and prepared at 200°C for 0.5 (d), 1 (e) and 2 (g) min.

space of bentonite. This result is consistent with the previous findings on solid-state ion exchange of zinc and copper with bentonite [20,23].

3.2. Dispersive X-ray spectroscopy

The result of elemental composition analysis is shown in Table 1. The parent bentonite is rich in calcium and its iron content is low (0.6%) which is included in the clay layers substituting either Al or Si. The composition of Fe at the Fe-B is increased to 6.9%–7.8% and the Ca and Mg is decreased to 0% after successful ion exchange with Fe. These results showed the exchangeable nature of calcium and manganese ions and the effectiveness of the ion exchange process. Potassium content for all samples is practically constant, indicating that this ion is not exchangeable. In the parent bentonite, some sulfur is also observed to result from an incomplete washing of bentonite by sulfuric acid in the manufacturer's unit. After ion exchange, no sulfur in the samples is observed, which results from the complete washing of the sample. Interestingly, the amount of calcium and magnesium in all samples was zero and the amount of iron in all samples reached a maximum value. This is due to the high speed ionic exchange reaction and its completion in a very short time of about 30 s. This time is much shorter than any research conducted on the basis of liquid ion exchange. In addition, the efficiency of the method is also very favorable and complete due to the amount of ion exchangeable ions being zeroed.

3.3. X-ray diffraction

XRD pattern for the parent bentonite and Fe-B is shown in Fig. 2. The peak at $2\theta = 6.30^\circ$ corresponds to the d_{001} basal spacing of 1.40 nm that is typical of calcium-rich montmorillonites and is in accordance with EDX data (Table 2). The peak of $2\theta = 20^\circ$ and the broad one nearby $2\theta = 35^\circ$ are the characteristic for smectites [18]. Those observed at $2\theta = 26.6^\circ$ and $2\theta = 20.8^\circ$ are assigned to quartz impurities. The XRD pattern of Fe-B suggests that after loading of Fe ions the clay mineral still holds the crystal structure of bentonite. In order to evaluate the ion exchange process efficiency, d_{001} basal spacing of the exchanged clays is presented in Table 2. As seen in this table, after ion

exchange, the 001 basal reflection has shifted to a higher angle. The diffraction peak at $2\theta = 6.30^\circ$ for parent bentonite, which corresponds to the d -spacing of 1.41 nm, shifted to $2\theta = 6.33^\circ$ – 6.84° , corresponding to an average interlayer distance of 1.27–1.36 nm. Thus, for the ion exchange samples, the (001) peak became narrower, its intensity increased, and the position shifted to a lower angles. It has been reported that this structural change is caused by loss of water present in the interlayer [19].

3.4. Discoloration tests

In this study, the MB photocatalytic degradation has been studied as a model dye. This dye is considered as one of the most toxic pollutants which is harmful to human health and water life [3]. The results showed that the degree of destruction of the synthesized samples at different times and temperatures is close to each other and after 120 min their efficiency is very close (Fig. 3). By comparing the discoloration efficiency for the synthesized samples, the amounts of degradation for samples 1, 2, 3, 4, 5, and 6 were 54.5%, 58.4%, 61.7%, 51.2%, 61.2%, and 57.2% after 10 min and they were around 100% after 120 min, which shows a small difference between the percent removal of the samples. It can be observed that the catalysts decolorization efficiency did not change significantly by the temperature and time of solid-state ion exchange progresses. This could be attributed to a number of factors including (1) same iron content and (2) same morphology.

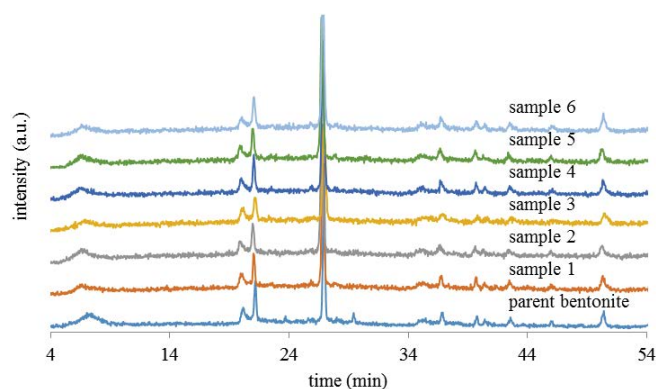


Fig. 2. XRD pattern of the parent bentonite and prepared Fe-B composites.

Table 1
Chemical composition of the parent bentonite and Fe-B

Element	Sample						
	0	1	2	3	4	5	6
O	55.9	45.9	46.1	46.7	46.2	45.7	46.1
Al	6.0	7.9	7.8	7.3	7.3	7.6	7.1
Si	28.8	37.1	37.2	38.0	37.9	37.7	38.4
K	1.4	1.3	1.4	1.2	1.4	1.3	1.2
Fe	0.6	7.8	7.7	6.9	7.2	7.7	7.4
Mg	1.0	0	0	0	0	0	0
S	3.3	0	0	0	0	0	0
Ca	2.9	0	0	0	0	0	0

Table 2
Basal spacing of the parent bentonite and Fe-B

Sample	2θ ($^\circ$)	d -spacing (\AA)
0	6.31	14.0128
1	6.54	13.51271
2	6.68	13.24028
3	6.91	12.79806
4	6.60	13.3976
5	6.61	13.36745
6	6.69	13.21045

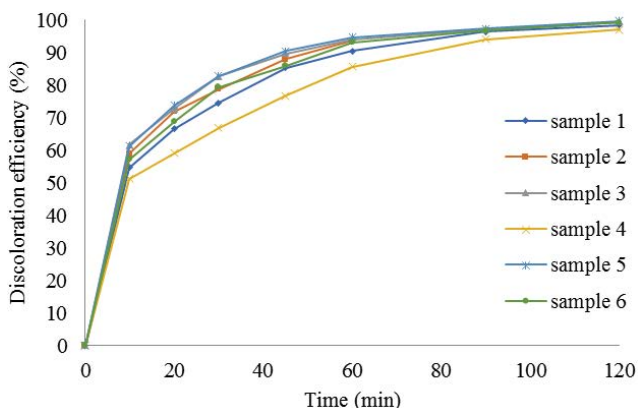


Fig. 3. Decolorization of 100 ppm MB by different prepared catalyst.

However, the rates of removal of the third (2 min at 100°C) and fifth samples (1 min synthesis at 200°C) are very close to each other and have the highest removal rate. With the convenience of achieving a temperature of 100°C as well as being close to the melting temperature of the used iron salt was sampled at 100°C for 2 min as an optimal sample. Among samples, the sample prepared at 100°C for 120 s was chosen as the optimum sample. The fewer temperature preferences are the reason for this.

Apparently, the decoloration kinetics of MB is significantly influenced by the experimental conditions. Without any H_2O_2 and catalyst, but with only 4 W UVC (Fig. 4a), the color removal is less than 5% after 120 min, indicating that the decoloration of 100 ppm MB can be ignored. This is because MB itself can resist UVC light, and direct photolysis of MB is very limited, which is consistent with previously published results [1]. In the absence of any catalyst and the presence of 10 mM H_2O_2 and 4 W UVC, the color removal approached 13% after 120 min. This is due to the fact that MB was oxidized by the OH radicals coming from direct photolysis of H_2O_2 in the presence of 4 W UVC. In the absence of UV light (dark) and 5 mM H_2O_2 but in the presence catalyst

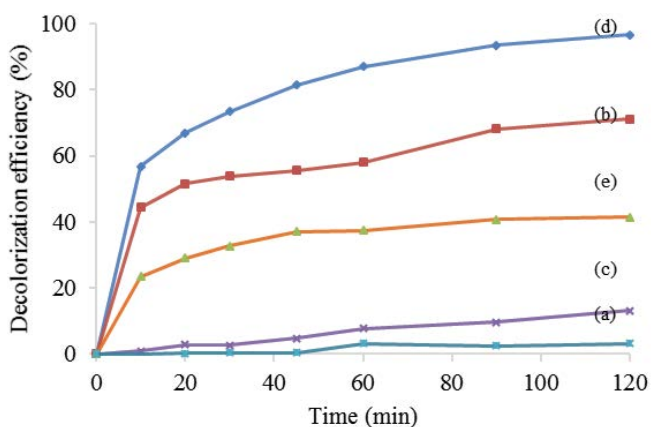


Fig. 4. Decoloration of 100 ppm MB under different conditions. (a) Only with 4 W UVC, (b) 10 mM H_2O_2 + 4 W UVC, (c) catalyst + 10 mM H_2O_2 + dark, (d) catalyst + 10 mM H_2O_2 + 4 W UVC, and (e) catalyst.

(Fig. 4c), the color removal of 100 ppm MB was less than 41% after 120 min reaction, indicating that the discoloration mechanism of 100 ppm MB is adsorption. This indicates that in the absence of UV light, the heterogeneous Fenton reaction itself is very slow, resulting in very limited OH radicals. With 4 W UVC, 10 mM H_2O_2 , and the catalyst (Fig. 4d), the color removal of 100 ppm MB was about 97% after 120 min reaction, illustrating that the catalyst exhibits good photocatalytic activity in the discoloration of 100 ppm MB in the presence of 4 W UVC light and 10 mM H_2O_2 .

The effect of the initial pH of the solution in MB dye decolorization is shown in Fig. 5. The contributory role of pH in a photo-Fenton process is very fundamental as it affects Fe activity and stability, H_2O_2 stability and the hydrolyzation of the HO and its activities. Fig. 5 shows that pH = 4 is the best for the decolorization of MB, which is in accordance with established trends in classical photo-Fenton process [18]. Discoloration decreased at pH = 4 and 5 the which indicates that the HO formation is being retarded due to the hydrolysis of Fe(III) and possible precipitation of FeOOH from the solution. Similar observations were obtained by several researchers as recently reviewed by Herney-Ramirez et al. [24].

The result of the effect of H_2O_2 concentration on the decolorization of MB in Fig. 6 shows that H_2O_2 concentration has significant effect on the efficiency of photo-Fenton process as earlier seen in Fig. 4. The best H_2O_2 dosage that decolorized

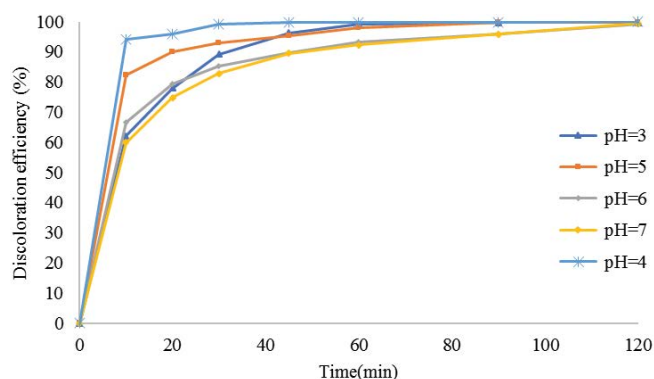


Fig. 5. Effect of initial pH on the decolorization of MB.

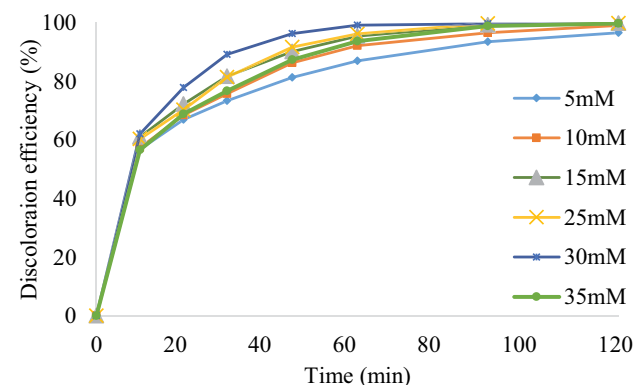


Fig. 6. Effect of H_2O_2 dosage on the decolorization of MB.

MB efficiently is 30 mM H_2O_2 . When the concentration is lower, the decolorization reduced because of insufficient H_2O_2 to generate the required HO. The decolorization was also reduced when the H_2O_2 concentration was increased to 35 mM, this can be explained by the possibility of scavenging of HO at higher concentrations of H_2O_2 [25]. This trend is also similar to other results [26].

Fig. 7 showed the result of catalyst loading in the decolorization of MB at the optimum pH and H_2O_2 dosage. The result is consistent with well known trend in photo-Fenton process, that is, increase in catalyst loading resulted in enhanced decolorization because of the availability of more catalyst active sites for hydroxylation of the HO and adsorption.

Fig. 8 shows the effect of different color concentrations on the decolorization efficiency. It is observed that increasing the color concentration from 100 to 400 ppm decreases the decolorization efficiency from 99% to 84% after 2 h. In high initial concentrations with constant radical hydroxyl concentration, the relative radical concentrations are low which reduces.

3.5. Catalyst reusability and leaching test

This test was conducted to evaluate the catalyst reuse. Fig. 9 showed the result of two reusability studies on the

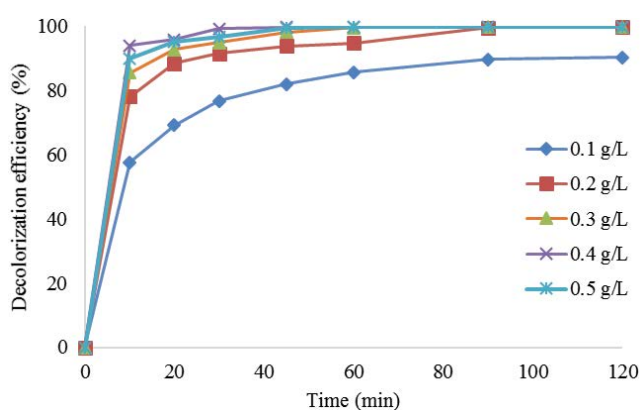


Fig. 7. Effect of the catalyst loading on the decolorization efficiency of MB.

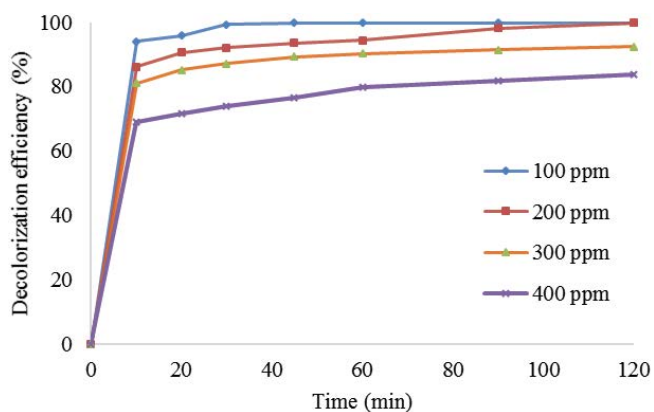


Fig. 8. Effect of methylene blue initial concentration in optimal operating conditions: 30 mM H_2O_2 and 0.4 g L^{-1} from the catalyst at pH 4.

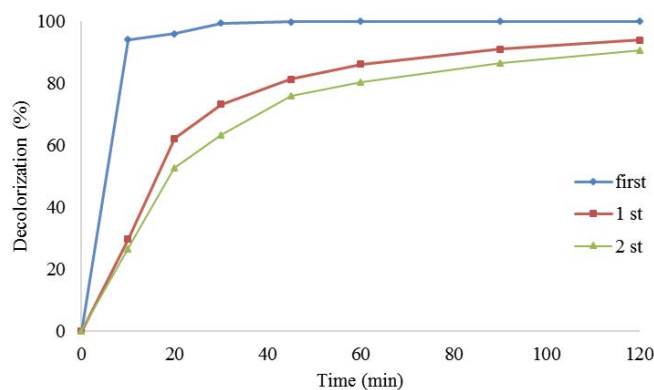


Fig. 9. Reuse of optimum prepared Fe-B composite for degradation of the methylene blue dye.

Catalyst for the decolorization of MB with 93.8% and 90.5% decolorization after 1st and 2nd reuse, respectively, during 120 min. The higher reusability of the catalyst can be related to its preparation protocols. In addition, the ability of the bentonite to provide sufficient sites for the Fe ion in the lamellare space provided a promising heterogeneous catalyst support for industrial application.

As shown in Fig. 9, the removal rate in the first 10 min of the catalytic reuse shows a drop, indicating high adsorption in the catalyst, after which, the rate of degradation in reuse has decreased by 29%, but after 120 min, this difference has dropped to 6%, which shows the use of Fe-B nanocomposite in photophantonic degradation as an effective way to reuse catalyst.

4. Conclusion

The aim of this study was the preparation and characterization of Fe-modified clays by solid ion exchange. The effects of reaction parameters such as initial dye concentration, H_2O_2 concentration, Fe-B catalyst loading and initial solution pH on the degradation of MB were also investigated. Between different prepared Fe-B catalysts, the sample prepared at 100°C and 2 min was selected as the optimum conditions for synthesis. Under Optimal conditions (pH = 4.0 and 200 ppm H_2O_2), ~100% discoloration of 200 ppm MB can be achieved in 90 min. The result of two reusability studies on the catalyst for the decolorization of MB was 93.8% and 90.5% after 1st and 2nd reuse, respectively.

References

- [1] M.A. De León, J. Castiglioni, J. Bussi, M. Sergio, Catalytic activity of an iron-pillared montmorillonitic clay mineral in heterogeneous photo-Fenton process, *Catal. Today*, 133 (2008) 600–605.
- [2] N. Wang, T. Zheng, G. Zhang, P. Wang, A review on Fenton-like processes for organic wastewater treatment, *J. Environ. Chem. Eng.*, 4 (2016) 762–787.
- [3] H.B. Hadjltaief, P. Da Costa, P. Beaunier, M.E. Gálvez, M.B. Zina, Fe-clay-plate as a heterogeneous catalyst in photo-Fenton oxidation of phenol as probe molecule for water treatment, *Appl. Clay Sci.*, 91 (2014) 46–54.
- [4] S. Lotfiman, M. Ghorbanpour, Antimicrobial activity of ZnO/silica gel nanocomposites prepared by a simple and fast solid-state method, *Surf. Coat. Technol.*, 310 (2017) 129–133.

- [5] N. Nasuha, S. Ismail, B.H. Hameed, Activated electric arc furnace slag as an efficient and reusable heterogeneous Fenton-like catalyst for the degradation of Reactive Black 5, *J. Taiwan Inst. Chem. Eng.*, 67 (2016) 235–243.
- [6] M. Ghorbanpour, M. Yousofi, S. Lotfiman, Photocatalytic decolorization of methyl orange by silica-supported TiO₂ composites, *J. Ultrafine Grained Nanostruct. Mater.*, 50 (2017) 43–50.
- [7] M. Ghorbanpour, S. Lotfiman, Solid-state immobilisation of titanium dioxide nanoparticles onto nanoclay, *Micro Nano Lett.*, 11 (2016) 684–687.
- [8] B.M. Zimmermann, S. Silvestri, J. Leichtweis, G.L. Dotto, E.S. Mallmann, E.L. Foletto, Effect of thermal treatment on the catalytic activity of a Fe-rich bentonite for the photo-Fenton reaction, *Cerâmica*, 65 (2019) 147–152.
- [9] B. Hakimi, M. Ghorbanpour, A. Feizi, A comparative study between photocatalytic activity of ZnO/bentonite composites prepared by precipitation, liquid-state ion exchange and solid-state ion exchange methods, *J. Water Environ. Nanotechnol.*, 3 (2018) 273–278.
- [10] J. Zhang, G. Liu, S. Liu, 2D/2D FeOCl/graphite oxide heterojunction with enhanced catalytic performance as a photo-Fenton catalyst, *New J. Chem.*, 42 (2018) 6896–6902.
- [11] N. Sétifi, N. Debbache, T. Sehili, O. Halimi, Heterogeneous Fenton-like oxidation of naproxen using synthesized goethite-montmorillonite nanocomposite, *J. Photochem. Photobiol., A*, 370 (2019) 67–74.
- [12] Z. Yang, A. Yu, C. Shan, G. Gao, B. Pan, Enhanced Fe(III)-mediated Fenton oxidation of atrazine in the presence of functionalized multi-walled carbon nanotubes, *Water Res.*, 137 (2018) 37–46.
- [13] M. Ghorbanpour, B. Hakimi, A. Feizi, A comparative study of photocatalytic activity of ZnO/activated carbon nanocomposites prepared by solid-state and conventional precipitation methods, *J. Nanostruct.*, 8 (2018) 259–265.
- [14] S.H. Bossmann, E. Oliveros, S. Göb, M. Kantor, A. Göppert, L. Lei, A.M. Braun, Degradation of polyvinyl alcohol (PVA) by homogeneous and heterogeneous photocatalysis applied to the photochemically enhanced Fenton reaction, *Water Sci. Technol.*, 44 (2001) 257–262.
- [15] Z.-r. Liu, S.-q. Zhou, Adsorption of copper and nickel on Na-bentonite, *Process Saf. Environ. Prot.*, 88 (2010) 62–66.
- [16] S. Louhichi, A. Ghorbel, H. Chekir, N. Trabelsi, S. Khemakhem, Properties of modified crude clay by iron and copper nanoparticles as potential hydrogen sulfide adsorption, *Appl. Clay Sci.*, 127 (2016) 123–128.
- [17] P. Yuan, H. He, F. Bergaya, D. Wu, Q. Zhou, J. Zhu, Synthesis and characterization of delaminated iron-pillared clay with meso-microporous structure, *Microporous Mesoporous Mater.*, 88 (2006) 8–15.
- [18] M.A. De León, M. Rodríguez, S.G. Marchetti, K. Sapag, R. Faccio, M. Sergio, J. Bussi, Raw montmorillonite modified with iron for photo-Fenton processes: influence of iron content on textural, structural and catalytic properties, *J. Environ. Chem. Eng.*, 5 (2017) 4742–4750.
- [19] M. Ghorbanpour, M. Mazloumi, A. Nouri, Silver-doped nanoclay with antibacterial activity, *J. Ultrafine Grained Nanostruct. Mater.*, 50 (2017) 124–131.
- [20] H. Pourabolghasem, M. Ghorbanpour, R. Shayegh, S. Lotfiman, Synthesis, characterization and antimicrobial activity of alkaline ion-exchanged ZnO/bentonite nanocomposites, *J. Central South Univ.*, 23 (2016) 787–792.
- [21] M. Ghorbanpour, Soybean oil bleaching by adsorption onto bentonite/iron oxide nanocomposites, *J. Phys. Sci.*, 29 (2018) 113–119.
- [22] A. Nouri, M. Ghorbanpour, S. Lotfiman, Diffusion of Cu ions into nanoclay by molten salt ion exchange for antibacterial application, *J. Phys. Sci.*, 29 (2018) 31–42.
- [23] H. Pourabolghasem, M. Ghorbanpour, R. Shayegh, Antibacterial activity of copper-doped montmorillonite nanocomposites prepared by alkaline ion exchange method, *J. Phys. Sci.*, 27 (2016) 1–12.
- [24] J. Herney-Ramirez, M.A. Vicente, L.M. Madeira, Heterogeneous photo-Fenton oxidation with pillared clay-based catalysts for wastewater treatment: a review, *Appl. Catal., B*, 98 (2010) 10–26.
- [25] O.S.N. Sum, J. Feng, X. Hub, P.L. Yue, Photo-assisted fenton mineralization of an azo-dye acid black 1 using a modified laponite clay-based Fe nanocomposite as a heterogeneous catalyst, *Top. Catal.*, 33 (2005) 233–242.
- [26] N.H.M. Azmi, O.B. Ayodele, V.M. Vadivelu, M. Asif, B.H. Hameed, Fe-modified local clay as effective and reusable heterogeneous photo-Fenton catalyst for the decolorization of Acid Green 25, *J. Taiwan Inst. Chem. Eng.*, 45 (2014) 1459–1467